Anisotropic Vector Hysteresis Model Using an Isotropic Vector Play Model

Tetsuji Matsuo[1], *Member, IEEE*

[1]Graduate School of Engineering, Kyoto University, Kyoto, 615-8510, Japan

A simple anisotropic vector hysteresis model is developed to represent 2D weakly anisotropic vector hysteretic property. An isotropic vector play model is identified from azimuthally averaged vector property of anisotropic material. An anisotropy matrix is multiplied to the isotropic vector play model to represent anisotropy. Simulations for alternating and rotational flux conditions show that the anisotropy matrix improves the representation of vector hysteretic properties for a non-oriented silicon steel sheet.

***Index Terms*—Alternating flux, anisotropic vector hysteresis, elliptically rotational flux, silicon steel sheet, vector play hysteron**

I. Introduction

THE PLAY model is an efficient and precise hysteresis model with two vector versions, respectively using superposition of scalar models along the azimuthal direction [1], [2] and a geometrically vectorized play hysteron [2]–[5]. The latter is the more efficient version because the former one requires azimuthal integration.

The isotropic rotational hysteretic property of a geometrically vectorized play model has been discussed in [2], [4], [5], in which several methods to adjust the simulated rotational hysteresis loss to the measured one have been proposed.

However, the representation of anisotropic vector hysteretic properties of silicon steel sheets remains as an open problem for the play model and other hysteresis models. Ref. [6] proposed an anisotropic vector hysteresis model using anisotropically vectorized stop hysterons. However, its identification is not an easy problem.

This paper presents a proposal of a simple generalization of vector play model for representation of the two-dimensional (2D) weakly anisotropic vector hysteretic property, which is observed in non-oriented steel sheets.

II. Isotropic Vector Play Model

An isotropic vector play model is given as the following.

$$\boldsymbol{H} = \boldsymbol{P}(\boldsymbol{B}) = \int_0^{B_S} \boldsymbol{f}(\zeta, \boldsymbol{p}_\zeta(\boldsymbol{B}))\mathrm{d}\zeta \tag{1}$$

$$\boldsymbol{f}(\zeta, \boldsymbol{p}) = f(\zeta, |\boldsymbol{p}|)\frac{\boldsymbol{p}}{|\boldsymbol{p}|} \tag{2}$$

Therein, $f(\zeta, \boldsymbol{p})$ is a shape function, B_S signifies the saturation magnetic flux density, and $\boldsymbol{p}_\zeta$ is a vector play hysteron of radius ζ. Hysteron $\boldsymbol{p}_\zeta$ [4] is given as presented below.

$$\boldsymbol{p}_\zeta(\boldsymbol{B}) = \boldsymbol{B} - \frac{\zeta(\boldsymbol{B} - \boldsymbol{p}_\zeta^{0*})}{\max(\zeta, |\boldsymbol{B} - \boldsymbol{p}_\zeta^{0*}|)} \tag{3}$$

$$\boldsymbol{p}_\zeta^{0*} = \frac{(B_S - \zeta)\boldsymbol{p}_\zeta^0}{\max(B_S - \zeta, |\boldsymbol{p}_\zeta^0|)} \tag{4}$$

Corresponding author: T. Matsuo (e-mail: tmatsuo@kuee.kyoto-u.ac.jp).

In those equations, $\boldsymbol{p}_\zeta^0$ is vector $\boldsymbol{p}_\zeta$ at the previous time-point.

The play model (1) is a 3D vector model. We discuss its 2D property to represent rotational and alternating hysteretic properties of silicon steel sheets.

The isotropic vector play model is identified as follows. An alternating magnetic flux density $\boldsymbol{B}_{alt}$ is given as

$$\boldsymbol{B}_{alt} = B_a\cos\omega t \ (\cos\varphi_B, \sin\varphi_B), \tag{5}$$

where B_a is the amplitude and φ_B is the azimuth angle. The angular frequency ω does not affect the property of the vector play model (1) because of its rate-independence. The alternating property $\boldsymbol{H}_{alt}(B, \varphi_B)$ for input (5) is

$$\boldsymbol{H}_{alt}(B_a\cos\omega t, \varphi_B) = \boldsymbol{H}(\boldsymbol{B}_{alt}) \ . \tag{6}$$

The averaged alternating property is given as

$$H_{ave}(B) = \frac{1}{\pi}\int_0^\pi \boldsymbol{H}_{alt}(B, \varphi)\cdot\boldsymbol{e}_\varphi \mathrm{d}\varphi \tag{7}$$

where $\boldsymbol{e}_\varphi$ is the unit vector in the φ-direction. Shape function f is determined from $H_{ave}(B)$ using the identification method for a scalar play model without the weighting function [7].

Alternating and rotational hysteretic properties of a non-oriented silicon steel sheet (JIS: 50A1300) are measured to examine the isotropic vector play model. The exciting frequency is 10 Hz and the eddy current influence is ignored. The dashed line in Fig. 1 shows the simulated rotational hysteresis loss per cycle of the steel sheet. It is larger than the measured value because the vector model is identified only from the alternating property above.

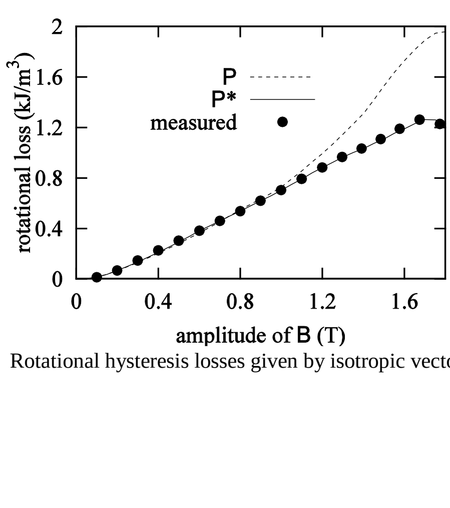

Fig. 1. Rotational hysteresis losses given by isotropic vector play models.

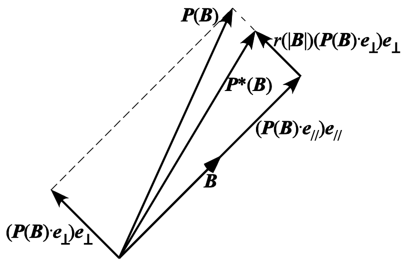

Fig. 2. Relation between $\boldsymbol{P}$ and $\boldsymbol{P}^*$.

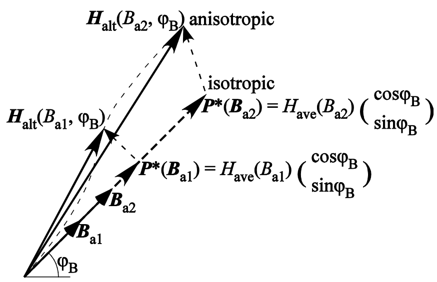

Fig. 3. Relation between $H_{\text{ave}}(B)$ and $\boldsymbol{H}_{\text{alt}}(B, \varphi_B)$.

Ref. [2] proposed an iterative method to adjust the simulated rotational loss to the measured one for the vector play model using a waiting function. This paper introduces another adjustment method without an iterative procedure, which has been applied to a vector stop model [8]. The vector play model is modified as

$$\boldsymbol{P}^*(\boldsymbol{B}) = (\boldsymbol{P}(\boldsymbol{B})\cdot\boldsymbol{e}_{//})\boldsymbol{e}_{//} + \boldsymbol{r}(|\boldsymbol{B}|)(\boldsymbol{P}(\boldsymbol{B})\cdot\boldsymbol{e}_{\perp})\boldsymbol{e}_{\perp} \tag{8}$$

where $\boldsymbol{e}_{//}$ and $\boldsymbol{e}_{\perp}$ respectively denote parallel and perpendicular unit vectors to $\boldsymbol{B}$, and $r(|\boldsymbol{B}|)$ is the ratio of the measured rotational hysteresis loss to the simulated loss given by $\boldsymbol{P}$. The relation between $\boldsymbol{P}$ and $\boldsymbol{P}^*$ is presented in Fig. 2. The solid line in Fig. 1 shows the rotational hysteresis loss given by $\boldsymbol{P}^*$, which agrees with the measured one.

III. Anisotropic Vector Hysteresis Model

A. Anisotropy Matrix Depending on B

A simple 2D anisotropic version of the vector play model is

$$\boldsymbol{P}_B(\boldsymbol{B}) = \boldsymbol{W}_B(\boldsymbol{B})\,\boldsymbol{P}^*(\boldsymbol{B})\,, \tag{9}$$

where $\boldsymbol{W}_B(\boldsymbol{B})$ is an anisotropy matrix of which components are single-valued functions of $\boldsymbol{B}$.

For example, $\boldsymbol{W}_B$ is determined to reconstruct the anisotropic alternating property approximately from the averaged alternating property as shown below.

$$\boldsymbol{W}_B(\boldsymbol{B}) = \begin{pmatrix} w_{Bx}(B,\varphi_B) & 0 \\ 0 & w_{By}(B,\varphi_B) \end{pmatrix} \tag{10}$$

$$w_{Bx}(B_{\text{a}},\varphi_B) = \frac{H_{\text{alt}x}(B_{\text{a}},\varphi_B)}{H_{\text{ave}}(B_{\text{a}})\cos\varphi_B}$$

$$w_{By}(B_{\text{a}},\varphi_B) = \frac{H_{\text{alt}y}(B_{\text{a}},\varphi_B)}{H_{\text{ave}}(B_{\text{a}})\sin\varphi_B} \tag{11}$$

Therein, $B = |\boldsymbol{B}|$ and $(H_{\text{alt}x}(B, \varphi_B), H_{\text{alt}y}(B, \varphi_B)) = \boldsymbol{H}_{\text{alt}}(B, \varphi_B)$ given by (6); the azimuthally averaged alternating property $H_{\text{ave}}(B)$ is assumed to be represented accurately by the isotropic vector play model $\boldsymbol{P}^*$. Both $\boldsymbol{H}_{\text{alt}}(B, \varphi_B)$ and $H_{\text{ave}}(B)$ are not single-valued functions but hysteretic functions. Accordingly, their amplitude properties are used in (11). The maximum point of alternating input $\boldsymbol{B}$ given by (5) with $\omega t = 0$ and the corresponding outputs of $\boldsymbol{H}_{\text{alt}}$ and H_{ave} are used to determine w_{Bx} and w_{By}. Fig. 3 shows the relation between $H_{\text{ave}}(B)$ and $\boldsymbol{H}_{\text{alt}}(B, \varphi_B)$.

B. Anisotropy Matrix Depending on P*

Another anisotropic vector play model is given as

$$\boldsymbol{P}_H(\boldsymbol{B}) = \boldsymbol{W}_H(\boldsymbol{P}^*)\,\boldsymbol{P}^*(\boldsymbol{B})\,, \tag{12}$$

where $\boldsymbol{W}_H$ is an anisotropy matrix of which components are single-valued functions of $\boldsymbol{P}^*$. For example, $\boldsymbol{W}_H$ is determined similarly to $\boldsymbol{W}_B$, as shown in the equations below.

$$\boldsymbol{W}_H(\boldsymbol{P}^*) = \begin{pmatrix} w_{Hx}(P^*,\varphi_H) & 0 \\ 0 & w_{Hy}(P^*,\varphi_H) \end{pmatrix} \tag{13}$$

$$w_{Hx}(H_{\text{ave}}(B_{\text{a}}),\varphi_B) = \frac{H_{\text{alt}x}(B_{\text{a}},\varphi_B)}{H_{\text{ave}}(B_{\text{a}})\cos\varphi_B}$$

$$w_{Hy}(H_{\text{ave}}(B_{\text{a}}),\varphi_B) = \frac{H_{\text{alt}y}(B_{\text{a}},\varphi_B)}{H_{\text{ave}}(B_{\text{a}})\sin\varphi_B} \tag{14}$$

The same relation between H_{ave} and $\boldsymbol{H}_{\text{alt}}(B, \varphi_B)$ as that for (11), illustrated in Fig. 3, is used for (14).

IV. Simulation Results

Vector hysteretic properties of the non-oriented silicon steel sheet (JIS: 50A1300) are simulated. Fig. 4 depicts components of $\boldsymbol{W}_B(\boldsymbol{B})$ and $\boldsymbol{W}_H(\boldsymbol{P}^*)$.

A. Alternating Magnetic Flux

Fig. 5 depicts alternating hysteretic properties of isotropic model $\boldsymbol{P}^*$ and anisotropic models $\boldsymbol{P}_B$ and $\boldsymbol{P}_H$ for $\varphi_B = 0, \pi/4, \pi/2$, where $H_{//} = \boldsymbol{H}\cdot\boldsymbol{e}_{//}$. The anisotropic models give accurate amplitudes of $H_{//}$. The discrepancy of alternating hysteretic properties between $\boldsymbol{P}_B$ and $\boldsymbol{P}_H$ is small.

B. Rotational Magnetic Flux

Figs. 6(a), 6(b), and 6(c) respectively portray the loci of $\boldsymbol{H}$ for counterclockwise rotational inputs of $\boldsymbol{B}$ with $|\boldsymbol{B}| = 0.5, 1.0, 1.5$ T, which are simulated respectively by $\boldsymbol{P}^*$, $\boldsymbol{P}_B$, and $\boldsymbol{P}_H$. The isotropic model $\boldsymbol{P}^*$ yields circular loci of $\boldsymbol{H}$. The loci obtained by $\boldsymbol{P}_B$ are directly affected by the phase lag of $\boldsymbol{B}$ to $\boldsymbol{P}^*$ because of $\boldsymbol{W}_B(\boldsymbol{B})$. The loci obtained by $\boldsymbol{P}_H$ are unaffected by the rotational direction because $\boldsymbol{W}_H(\boldsymbol{P}^*)$ does not depend on the phase lag of $\boldsymbol{B}$ to $\boldsymbol{P}^*$. In other words, the anisotropy in $\boldsymbol{P}_B$ depends only on $\boldsymbol{B}$, although that in $\boldsymbol{P}_{\text{H}}$ depends only on $\boldsymbol{P}^*$.

To incorporate dependences on $\boldsymbol{B}$ and $\boldsymbol{P}^*$, another simple anisotropic model is introduced as

$$\boldsymbol{P}_{BH}(\boldsymbol{B}) = \boldsymbol{W}_{BH}(\boldsymbol{B}, \boldsymbol{P}^*)\,\boldsymbol{P}^*(\boldsymbol{B}) \tag{15}$$

$$\boldsymbol{W}_{BH}(\boldsymbol{B}, \boldsymbol{P}^*) = \{\, \boldsymbol{W}_B(\boldsymbol{B}) + \boldsymbol{W}_H(\boldsymbol{P}^*) \,\} / 2\,. \tag{16}$$

Fig. 6(d) portrays loci of $\boldsymbol{H}$ given by $\boldsymbol{P}_{BH}(\boldsymbol{B})$, which approximately agrees with the measured loci.

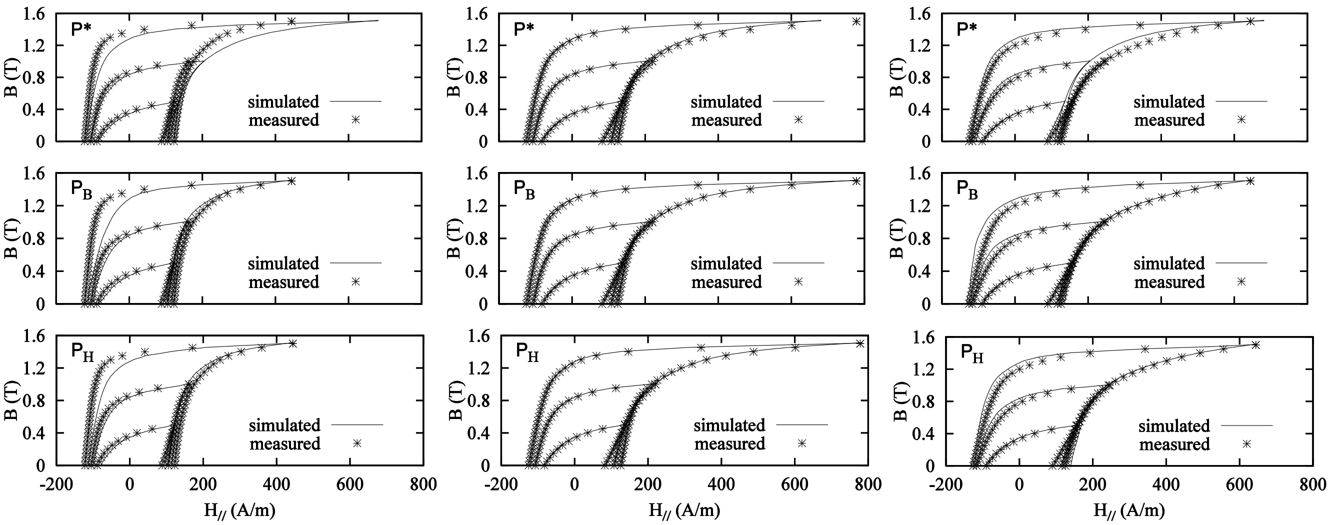

(a) (b) (c)

Fig. 5. Alternating hysteretic properties of isotropic model $\boldsymbol{P}^*$ and anisotropic models $\boldsymbol{P}_B$ and $\boldsymbol{P}_H$: (a) $\varphi_B = 0$, (b) $\varphi_B = \pi/4$, and (c) $\varphi_B = \pi/2$.

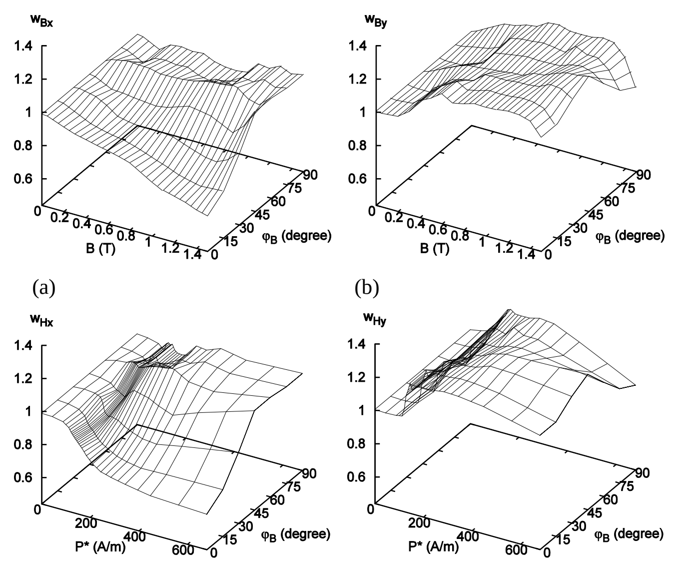

(a) (b) (c) (d)

Fig. 4. Components of anisotropy matrices: (a) w_{Bx}, (b) w_{By}, (c) w_{Hx}, and (d) w_{Hy}.

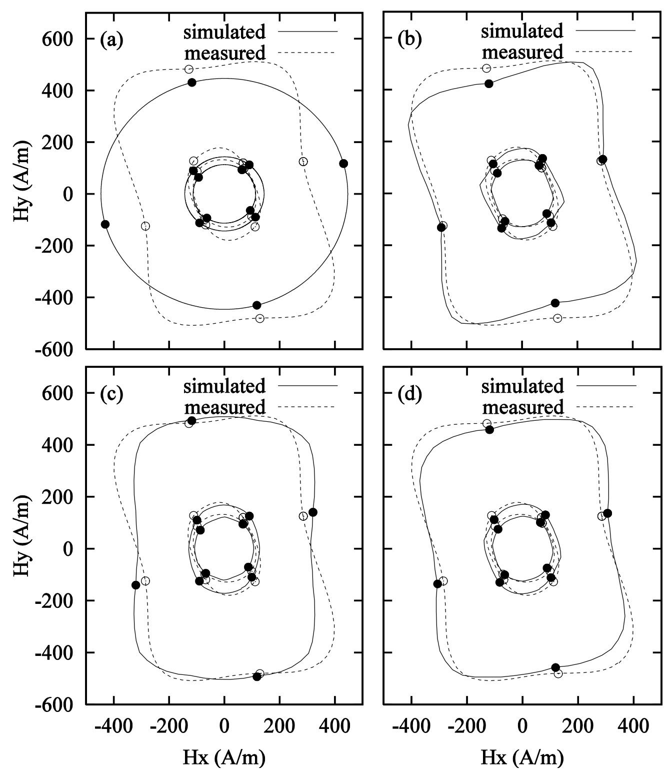

Fig. 6. Simulated loci of $\boldsymbol{H}$ for rotational inputs of $\boldsymbol{B}$, where $B_x = 0$ or $B_y = 0$ at "•" (simulated) and "o" (measured): (a) $\boldsymbol{H} = \boldsymbol{P}^*$, (b) $\boldsymbol{H} = \boldsymbol{P}_B$, (c) $\boldsymbol{H} = \boldsymbol{P}_H$, and (d) $\boldsymbol{H} = \boldsymbol{P}_{BH} = (\boldsymbol{P}_B + \boldsymbol{P}_H)/2$.

C. Elliptically Rotational Magnetic Flux

The vector hysteretic property for elliptically rotational magnetic flux is examined. Fig. 7 depicts the loci of elliptically rotational magnetic flux density where the major radius $B_M \approx$ 0.5, 1.0, and 1.5 T and the azimuth angle of major axis $\varphi_M = 0$, $\pi/4$, and $\pi/2$. Fig. 8 shows the corresponding loci of $\boldsymbol{H}$ that are simulated by $\boldsymbol{P}^*$ and $\boldsymbol{P}_{BH}$ for counterclockwise rotation. The isotropic model $\boldsymbol{P}^*$ yields loci of $\boldsymbol{H}$ that qualitatively agree with measured loci. The anisotropic model $\boldsymbol{P}_{BH}$ achieves more accurate representation than $\boldsymbol{P}^*$ does.

V. Conclusion

A simple anisotropy matrix improves the representation of the vector hysteretic properties of non-oriented silicon steel sheet. The anisotropy matrices examined herein are too simple for highly accurate representation. Future work should be done to improve the anisotropy matrix identification method.

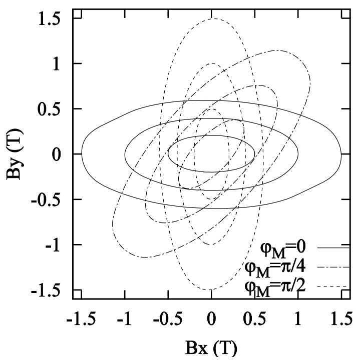

Fig. 7. Loci of elliptically rotational magnetic flux density, where φ_M is the azimuth angle of the major axis.

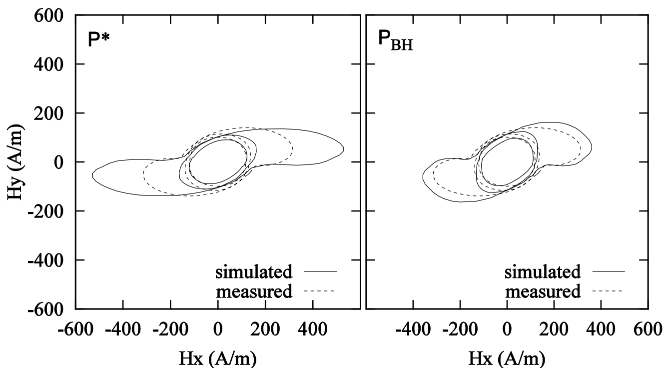

(a)

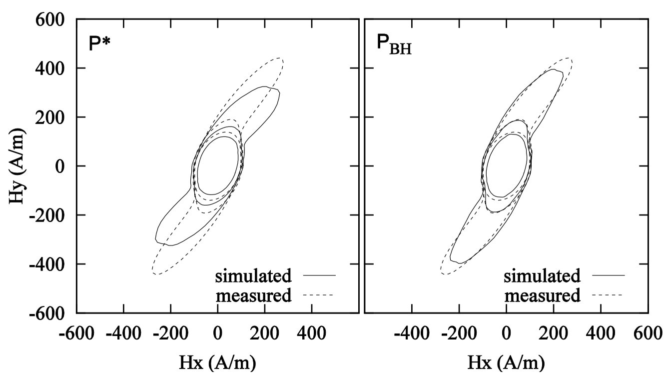

(b)

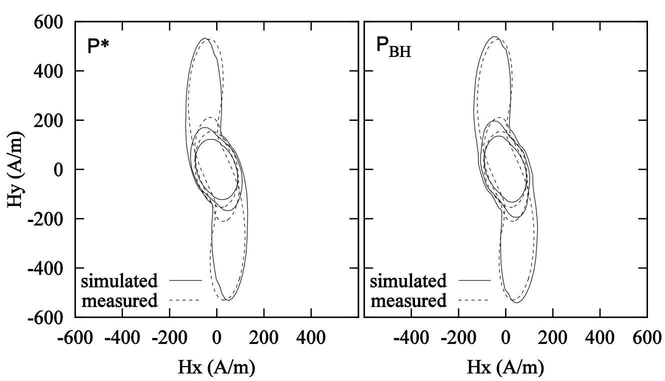

(c)

Fig. 8. Loci of $\boldsymbol{H}$ simulated by $\boldsymbol{P}^*$ (left) and $\boldsymbol{P}_{BH}$ (right) for counterclockwise elliptically rotational inputs of $\boldsymbol{B}$: (a) $\varphi_M = 0$, (b) $\varphi_M = \pi/4$, and (c) $\varphi_M = \pi/2$.

ACKNOWLEDGMENT

The author expresses his gratitude to his graduate students, Mr. H. Kaneda and Mr. M. Miyamoto, Kyoto University, Japan for measurement of magnetic properties of silicon steel sheets. The author also thanks Dr. C. Lee and Dr. K. Miyata, Hitachi, Ltd. for useful discussions of vector hysteresis. This work was supported in part by the Japan Society for the Promotion of Science, Grant-in-Aid for Scientific Research (C), 19560288.

REFERENCES

[1] T. Matsuo, Y. Osaka, and M. Shimasaki, “Eddy-current analysis using vector hysteresis models with play and stop hysterons,” *IEEE Trans. Magn.*, vol. 36, pp. 1172-1177, July 2000.

[2] T. Matsuo and M. Shimasaki, “Two types of isotropic vector play models and their rotational hysteresis losses,” *IEEE Trans. Magn.*, vol. 44, pp. 898-901, June 2008.

[3] A. Bergqvist, “Magnetic vector hysteresis model with dry friction-like pinning,” *Physica B*, vol. 233, pp. 342-347, 1997.

[4] C. Serpico, M. d'Aquino, C. Visone and D. Davino, “A new class of Preisach-type isotropic vector model of hysteresis,” *Physica B*, vol. 343, pp. 117-120, 2004.

[5] T. Matsuo, “Rotational saturation properties of isotropic vector hysteresis models using vectorized stop and play hysterons,” *IEEE Trans. Magn.*, vol. 44, pp. 3185-3188, Nov. 2008.

[6] J.V. Leite, N. Sadowski, P. Kuo-Peng, and J.P.A. Bastos, “A new anisotropic vector hysteresis model based on stop hysterons,” *IEEE Trans. Magn.*, vol. 41, pp. 1500-1503, May 2005.

[7] T. Matsuo and M. Shimasaki, “An identification method of play model with input-dependent shape function,” *IEEE Trans. Magn.*, vol. 41, pp. 3112-3114, Oct. 2005.

[8] T. Matsuo, “Comparison of rotational hysteretic properties of isotropic vector stop models,” *IEEE Trans. Magn.*, vol. 45, pp. 1194-1197, March 2009.